Hydrodynamic and environmental characteristics of a tributary bay influenced by backwater jacking and intrusions from a main reservoir

Xintong Li[1], Bing Liu[2], Yuanming Wang[1], Yongan Yang[3], Ruifeng Liang[1]*, Fangjun Peng[1], Shudan Xue[1], Zaixiang Zhu[1], Kefeng Li[1]

[1] *State Key Laboratory of Hydraulics and Mountain River Engineering, Sichuan University, Chengdu 610065, China*

[2] *Emergency Response Centre, Ecology and Environment Bureau of Suining, Suining 629000, China*

[3] *Environmental Monitoring Centre, Ecology and Environment Bureau of Suining, Suining 629000, China*

Abstract. The construction of large reservoirs results in the formation of tributary bays, and tributary bays are inevitably influenced by backwater jacking and intrusions from the main reservoir. In this paper, a typical tributary bay (Tangxi River) of the Three Gorges Reservoir (TGR) was selected to study the hydrodynamic and environmental characteristics of a tributary bay influenced by the jacking and intrusions from the main reservoir. The flow field, water temperature and water quality of the Tangxi River were simulated using the hydrodynamic and water quality model CE-QUAL-W2, and the eutrophication status of the tributary bay was also evaluated. The results showed that the main reservoir had different effects on its tributary bay in each month. The tributary bay was mainly affected by backwater jacking from the main reservoir when the water level of the main reservoir dropped and by intrusions from the main reservoir when the water level of the main reservoir rose. An obvious water quality concentration boundary existed in the tributary bay, which was basically consistent with the regional boundary in the flow field. The flow

field and water quality on both sides of the boundary were quite different. The results of this study can help us figure out how the backwater jacking and intrusions from the main reservoir influence the hydrodynamic and water environment characteristics of the tributary bay and provide guidance for water environment protection in tributary bays.

Keywords: tributary bay, main reservoir, backwater jacking, intrusion, hydrodynamic conditions, environmental factors

1 Introduction

The functions of water conservancy and hydropower projects include power generation, flood control, irrigation and shipping, which play an important role in human social life (Deng and Bai, 2016; Zhang, 2014; Peng, 2014). In recent years, a large number of high dams, with heights of even 300 m, have been planned or completed in the middle and upper reaches of the Yangtze River to meet the increasing energy demand (Zhou et al., 2013). These dams block fish migration routes between upstream and downstream regions (Oldani and Claudio, 2002; Ziv et al., 2012) and change the fish communities (Gao et al., 2010). In the flood season, flood discharge produces water that is supersaturated in dissolved gas in the downstream river channel (Feng et al., 2014; Lu et al., 2011; Wang et al., 2011; McGrath, 2006). In the reservoir area, the elevated water level produces a much slower water velocity, which results in sediment deposition, eutrophication, and stratification in terms of water temperature and water quality (Zhu, 2017; Wu, 2013; Zhang et al., 2011).

Backwater extends to some tributaries after the construction of dammed-river reservoirs, which causes the water depth to increase and the water velocity to slow in these tributaries, thus forming water areas similar to lakes known as a tributary bay (Yu et al., 2013). Backwater areas represent the connection between different habitats in the main stream and the tributary and are also an important location for physical, chemical and biological exchanges between adjacent habitats (Zhang et al., 2010). After the impoundment of a reservoir, the hydrodynamic conditions and the environmental factors (water temperature, water quality, etc.) of the tributaries in the reservoir area are affected by the main stream and exhibit complex distribution characteristics (Xiong et al., 2013). Backwater jacking occurs in tributaries when dams or other obstructions raise the surface of the water upstream from them. Intrusion is the process by which water from the mainstream intrudes into the tributary. A tributary bay is always influenced by backwater jacking and intrusions under fluctuations of the water level of the main reservoir because such changes induce changes in the hydrodynamic conditions in the tributary bay (Ji et al., 2010; Wang et al., 2014). The velocity of water in the horizontal direction becomes uneven, and the velocity on the side near the confluence is obviously higher than that on the other side (Hu et al., 2013; Yin et al., 2013). The flow field distribution tends to gradually change with increasing distance from the confluence (Yin et al., 2013). The water level of a reservoir changes constantly to meet multiple requirements, which results in changes in water temperature and water environment in tributary bays (Fu et

al., 2010; Holbach et al., 2013; Yang et al., 2013). Existing studies have shown that water level fluctuation has become a major cause of recent eutrophication and pollution problems in the Three Gorges Reservoir (TGR), particularly within its tributary backwaters (Holbach et al., 2015). After the impoundment of reservoirs, eutrophication and eutrophication-related problems often occur in tributary bays due to changes in nutrient patterns (Yang et al., 2010; Liu et al., 2012; Ran et al., 2019). Therefore, exploring the distribution and evolution of the hydrodynamic and water environment characteristics of tributary bays in response to backwater jacking and intrusions from the main reservoir is a key to solving eutrophication problems.

Many recent studies have paid attention to the deterioration of the water environment in tributary bays. In response to the operation of cascade reservoirs, a series of profound geological, morphological, ecological, and biogeochemical responses will appear in the estuary, delta, and coastal sea of the Yangtze River subaqueous delta (Hu et al., 2009). Some scholars have found that the water quality of the TGR was relatively stable before and after impoundment but that the water quality of tributary bays deteriorated, resulting in frequent algal blooms (Liu et al., 2016; Zou and Zhai, 2016; Cai and Hu, 2006). Changes in the vertical mixing of layers driven by stratified density currents were the key factor in the formation of algal blooms (Tang et al., 2016; Zhang et al., 2015). Through isotopic measurements in the Xiangxi River or other tributaries of the TGR, it has been found that the nutrients in tributary bays did not originate solely in the tributary basins but instead were mainly from the main

85 stream of the Yangtze River and that the nutrient levels were affected by constantly
86 changing hydrodynamic conditions across seasons (Holbach et al., 2014; Yang et al,
87 2018; Zheng et al., 2016). A rise in the water level may lead to a rise or decline in the
88 chlorophyll content depending on the water cycle mode in the tributary (Ji et al.,
89 2017). Previous studies have paid considerable attention to changes in hydrodynamic
90 characteristics and the deterioration of the water environment in the tributaries but
91 have not considered the influence of the main reservoir (Zhao, 2017; Long et al.,
92 2019). There are few systematic studies on the variation in the hydrodynamic and
93 water environment characteristics of tributary bays influenced by backwater jacking
94 and intrusions from the main reservoir. There are many open questions regarding the
95 functions of these types of systems: How does the operation of the main reservoir
96 affect tributary bays? How do hydrodynamic forces and the water environment of
97 tributary bays respond to backwater jacking and the intrusion of water from the main
98 reservoir? What controls the water environment of tributary bays? These questions
99 have not yet been resolved.

100 The Tangxi River is a typical tributary bay of the TGR, and it has been severely
101 influenced by backwater jacking and intrusions in recent years. This phenomenon
102 accelerates the deterioration of the water environment of Tangxi River. Thus, the
103 Tangxi River was selected as the focus of this study. Based on the collection and
104 analysis of basic data, we simulated the flow field, water temperature, and water
105 quality of the Tangxi River using the hydrodynamic and water quality model

106 CE-QUAL-W2. This model performs well in computing the velocity, the intrusion
107 layer at the plunge point, and the travel distance of the density-driven current (Long et
108 al., 2019), and many scholars have obtained good results using this model to simulate
109 the hydrodynamics, water temperature and water quality of reservoirs and lakes
110 (Bowen and Hieronymus, 2003; Lung and Nice, 2007; Berger and Wells, 2008;
111 Debele et al., 2008; Noori, 2015; Long et al., 2018). We also evaluated the
112 eutrophication status of the tributary bay and systematically identified the influence of
113 backwater jacking and intrusions from the main reservoir on the tributary bay. The
114 results of this study can help us to figure out how the backwater jacking and
115 intrusions from the main reservoir influenced the hydrodynamic and water
116 environment characteristics of the tributary bay and provide guidance for water
117 environment protection in tributary bays.

118 **2 Materials and methods**

119 **2.1 Research area**

120 The main stream of the Yangtze River has a total length of approximately 6300 km
121 and a drainage area of approximately 1.8 million km^2. The reach between Yichang
122 City and Hubei Yibin City in Sichuan is considered the upper reaches of the Yangtze
123 River, which has a length of 1045 km and a natural drop of 220 m. The drainage area
124 of the upper Yangtze River is 527000 km^2, and its average annual flow is 14300 m^3/s
125 (Fan, 2007).

126 The Tangxi River is a first-order tributary of the upper Yangtze River and has a

total length of 104 km, a drainage area of 1707 km^2 and an average annual flow of 57.2 m^3/s. After the completion of the TGR, the Tangxi River became a tributary bay of the TGR. In this paper, the 42.6 km long reach of the Tangxi River affected by the backwater jacking and intrusions from the TGR was selected as the study area (Fig.1).

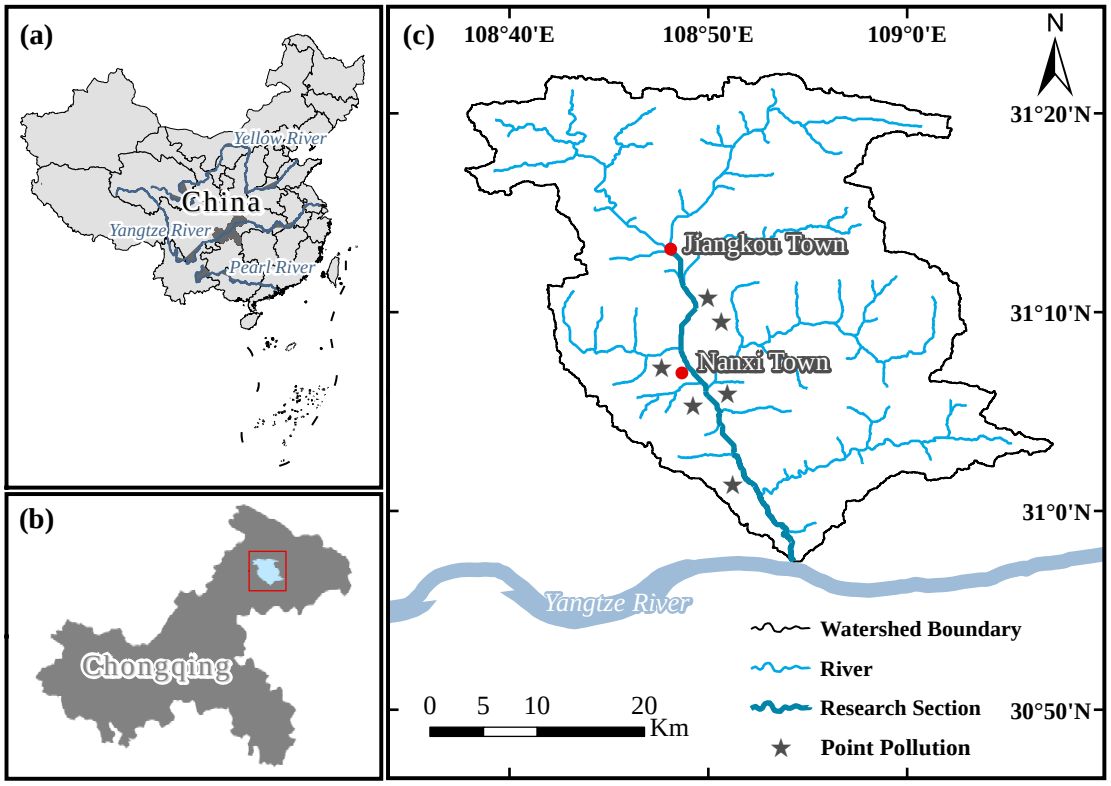

Fig. 1. Research area and hydrologic system of the Tangxi River Basin. (a) Location of the research area relative to China; (b) Location of the research area relative to Chongqing; (c) Hydrologic system of the research area.

2.2 Numerical simulation of hydrodynamic and environmental factors in the tributary bay

2.2.1 Mathematical model

The vertical two-dimensional model CE-QUAL-W2 solves the width averaged

equations and is appropriate for simulating flow in long narrow water bodies. This model was adopted for the calculation of the hydrodynamic conditions, water temperature and water quality in the tributary bay (Thomas and Scott, 2008). The model is solved by coupling governing equations, a transport equation and a surface heat exchange equation. The research river was divided into 107 × 38 (longitudinal × vertical) rectangular cell grids with a longitudinal dimension of 400 m and vertical dimension of 2 m (Fig. 2).

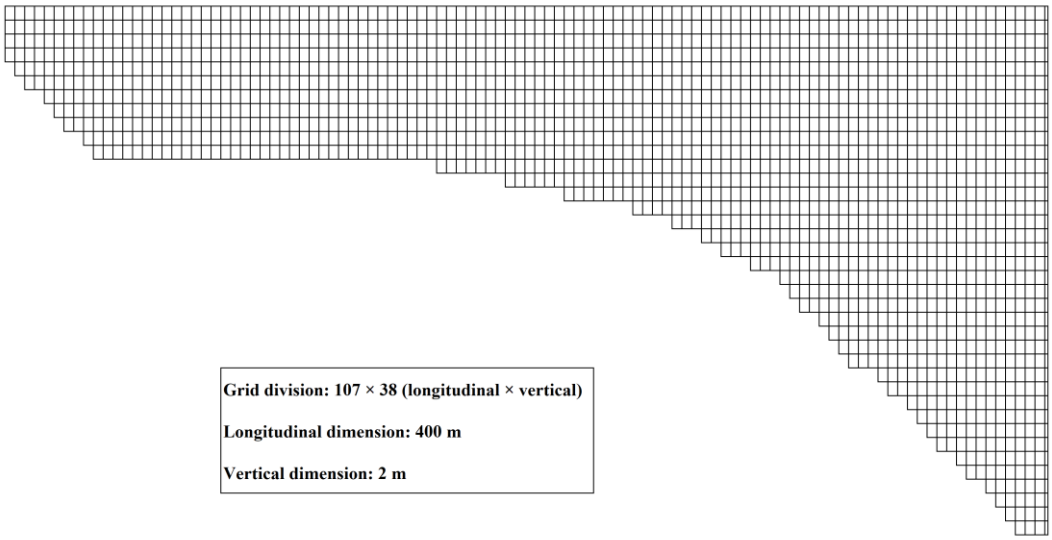

Fig. 2. Grid structure of the research area.

The governing equations of the model are as follows.

The continuity equation:

$$\frac{\partial UB}{\partial x} + \frac{\partial WB}{\partial z} = qB \tag{1}$$

The x-momentum equation:

$$\frac{\partial UB}{\partial t} + \frac{\partial UUB}{\partial x} + \frac{\partial WUB}{\partial z} = gB\,sin\,\alpha - \frac{B}{\rho}\frac{\partial P}{\partial x} + \frac{1}{\rho}\frac{\partial B\tau_{xx}}{\partial x} + \frac{1}{\rho}\frac{\partial B\tau_{xz}}{\partial z} \tag{2}$$

The z-momentum equation:

$$\frac{1}{\rho}\frac{\partial P}{\partial z} = g\cos\alpha \quad (3)$$

The free water surface equation:

$$B_\eta \frac{\partial \eta}{\partial t} = \frac{\partial}{\partial x}\int_\eta^h UB\,dz - \int_\eta^h qB\,dz \quad (4)$$

The equation of state:

$$\rho = f(T_W, \Phi_{TDS}, \Phi_{ISS}) \quad (5)$$

where x and z represent the horizontal distance and vertical elevation, respectively; U and W are the temporal mean velocity components in the horizontal and vertical directions; B is the channel width; q is the discharge; t denotes the time; g is the acceleration of gravity; α is the angle of the riverbed with respect to the x-direction; P represents pressure; τ_{xx} and τ_{xz} are the lateral average shear stress in the x-direction and z-direction, respectively; ρ represents density; η and h are the water surface and water depth, respectively; and $f(T_W, \Phi_{TDS}, \Phi_{ISS})$ is a density function dependent upon temperature, total dissolved solids or salinity, and inorganic suspended solids.

Accurate hydrodynamic calculations require accurate water densities. The following equation of state relating the density to the water temperature was used in the model:

$$\rho_{Tw} = 999.845259 + 6.793952\times10^{-2}T_w - 9.19529\times10^{-3}T_w^2 + 1.001685\times10^{-4}T_w^3 - 1.120083\times10^{-6}T_w^4 + 6.536332\times10^{-9}T_w^5 \quad (6)$$

where ρ_{Tw} denotes density and T_W is the water temperature.

The universal transport equation for scalar variables, such as temperature and

chemical oxygen demand (COD), is as follows:

$$\frac{\partial B\Phi}{\partial t}+\frac{\partial UB\Phi}{\partial x}+\frac{\partial WB\Phi}{\partial z}-\frac{\partial\left(BD_x\frac{\partial\Phi}{\partial x}\right)}{\partial x}-\frac{\left(BD_z\frac{\partial\Phi}{\partial z}\right)}{-\partial z}=q_\Phi B+S_\Phi B \quad (7)$$

where Φ is the laterally averaged constituent concentration; D_x and D_z are the temperature and constituent dispersion coefficient in the horizontal and vertical directions, respectively; q_Φ represents the lateral inflow or outflow mass flow rate of the constituent per unit volume; and S_Φ denotes the laterally averaged source/sink term.

Heat exchange at the water surface includes net solar shortwave radiation, net longwave radiation, evaporation and conduction. The surface heat exchange is computed as follows:

$$H_n=H_s+H_a+H_e+H_c-(H_{sr}+H_{ar}+H_{br}) \quad (8)$$

where H_n is the net rate of heat exchange across the water surface; H_s is the incident shortwave solar radiation; H_a represents the incident longwave radiation; H_{sr} and H_{ar} represent the reflected solar radiation of shortwave and longwave radiation, respectively; H_{br} is the back radiation from the water surface; H_e is the evaporative heat loss; and H_c represents the heat conduction.

The shortwave absorption model we used was based on Bears Law (Thomas and Scott, 2008). The attenuation coefficients in the model include the fraction absorbed at the water surface and the extinction coefficient, which were 0.45 and 0.45 m^{-1}, respectively. Due to the exponential decay of the shortwave radiation, we did not distinguish the heating after radiation reached the bottom of the tributary in the

196 simulation.

197 **2.2.2 Model validation**

198 The water quality at the Tangxi River Bridge was monitored in 2017, and the data was
199 used to verify the model and the degradation coefficient of each water quality
200 parameter. The Tangxi River Bridge is 18 km from the confluence. Due to the low
201 water level of the main reservoir, the backwater did not reach the Tangxi River Bridge
202 from June to August. Therefore, only the data from January to May and from
203 September to December were selected to verify the simulated results of water
204 temperature (T), ammonia nitrogen (NH_3-N), total phosphorus (TP), and total
205 nitrogen (TN). COD values were not measured. The degradation coefficients of COD，
206 NH_3-N, TP and TN are 0.0032 d^{-1}, 0.0032 d^{-1}, 0.0018 d^{-1}, and 0.0018 d^{-1} respectively .

207 The results showed that the simulated values of T, TP and TN fit well with the
208 measured values. The difference in T between the simulated value and the measured
209 value was 0.6 - 4.7 ºC, and the root mean squared error was 1.8 ºC. The difference in
210 TP between the simulated value and the measured value was 0.004 - 0.03 mg/L, and
211 the root mean squared error was 0.01 mg/L. The difference in TN between the
212 simulated value and the measured value was 0.02 - 0.26 mg/L, and root mean squared
213 error was 0.16 mg/L. For NH_3-N, the difference between the simulated value and the
214 measured value was 0.03 - 0.08 mg/L, the root mean squared error was 0.06 mg/L,
215 and the relative error was greater than 30%. The degradation process of NH_3-N
216 usually exhibits complex characteristics, and many factors affect the degradation

coefficient of NH_3-N, such as the water microbial properties, hydrodynamic conditions, water pollution degree, suspended solids and pH (Bockelmann et al., 2004; Wang et al., 2016; Pan et al., 2020), which resulted in a higher simulation error compared with the other values.

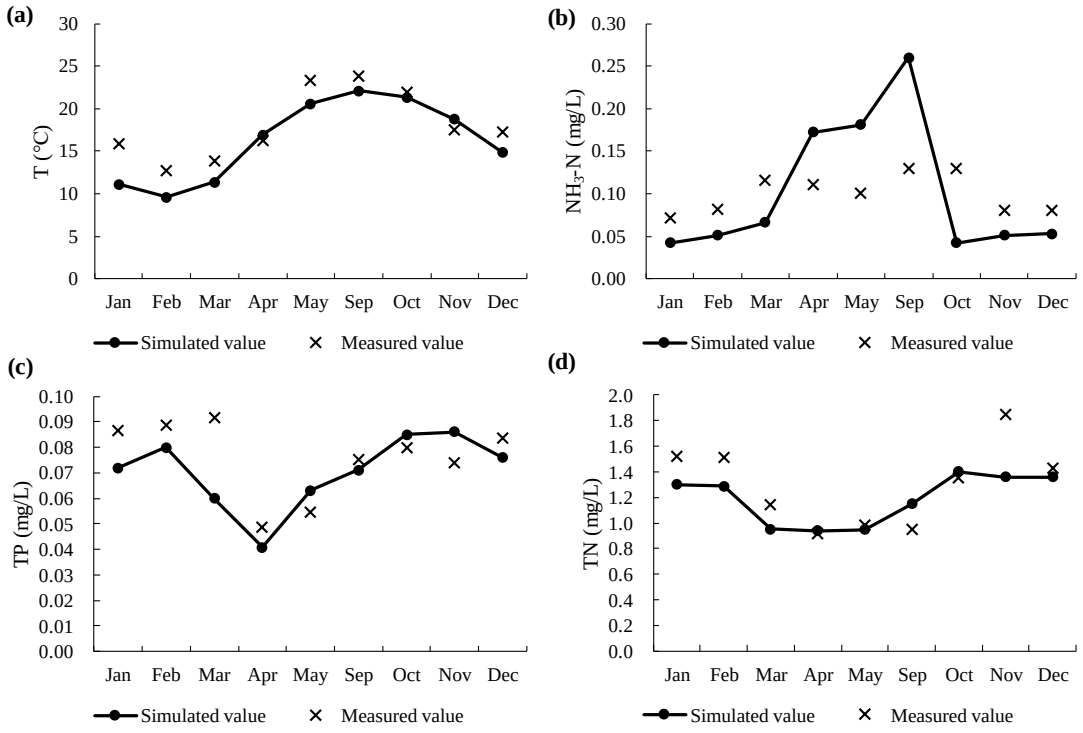

Fig. 3. Comparison between the simulated and measured values at the Tangxi River Bridge in each month. (a) Comparison of water temperature; (b) Comparison of ammonia nitrogen; (c) Comparison of total phosphorus; (d) Comparison of total nitrogen.

2.2.3 Boundary conditions

The boundary conditions of the calculation included the meteorology, water temperature of the inflow, discharge flow, water quality and water level of the TGR. The daily average multi-year meteorological data (2011-2018) were obtained from

Yunyang County weather station, which is 19.7 km away from the tributary bay (Fig. 4). The pollution loads of point and non-point sources were calculated and included as inputs to the numerical simulations (Table 1). The daily average multi-year data on the boundary conditions of flow, water level, water temperature and water quality were also considered (Fig. 5). The diurnal cycle of the simulation lasted three years.

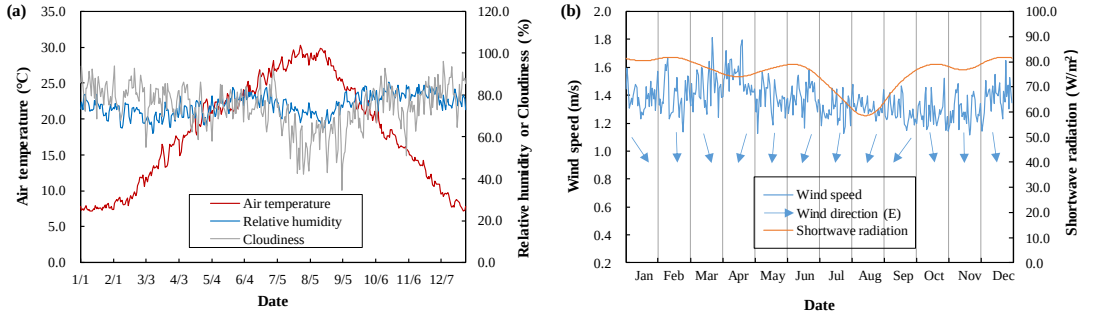

Fig. 4. Meteorological conditions. (a) Daily average multi-year values of air temperature, humidity and cloudiness and (b) daily average multi-year values of wind conditions and shortwave radiation.

Table 1.

Statistics of pollution load in the Tangxi River research area.

Factors	COD (t/a)		NH_3-N (t/a)		TP (t/a)		TN(t/a)	
	Point	Non-point	Point	Non-point	Point	Non-point	Point	Non-point
Pollution Load	2093.58	1537.35	354.21	154.46	35.08	23.90	2093.58	1537.35

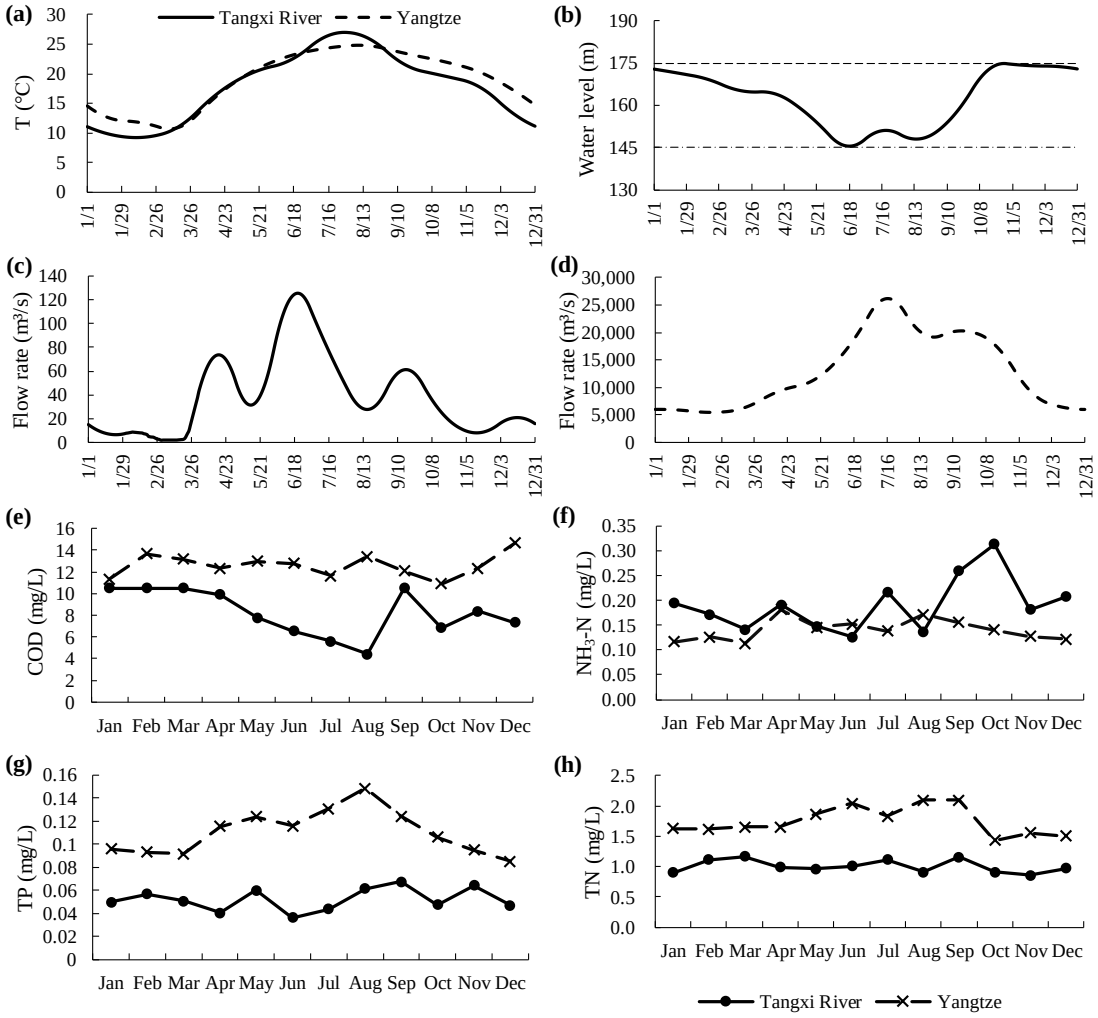

Fig. 5. Simulation boundary conditions. (a) Daily water temperatures of the main reservoir and tail of the tributary bay; (b) Water level of the main reservoir, (c) Daily inflow of the tributary bay; (d) Daily inflow of the main reservoir; (e) - (h) Monthly water quality (COD, NH_3-N, TP and TN) of the main reservoir and tributary bay, respectively.

2.3 Simulation of eutrophication

The comprehensive nutrition index (*TLI* (∑)) method (Carlson, 1977) was used to evaluate the nutritional status of the tributary bay. Lakes and reservoirs can be classified into different nutritional statuses based on their *TLI* (∑) values:

$TLI(\sum) < 30$, oligotrophic

$30 \leq TLI(\sum) \leq 50$, mesotrophic

$TLI(\sum) > 50$, eutrophic

$50 < TLI(\sum) \leq 60$, slightly eutrophic

$60 < TLI(\sum) \leq 70$, moderately eutrophic

$TLI(\sum) > 70$, severely eutrophic

The formula for calculating the $TLI(\sum)$ is as follows:

$$TLI(\sum) = \sum_{j=1}^{m} W_j \cdot TLI(j) \quad (9)$$

where $TLI(\sum)$ is the comprehensive nutrition index; W_j represents the correlation weight of the nutrition state index of the *j*-th parameter; and $TLI(j)$ denotes the nutritional status index of the *j*-th parameter.

Considering chlorophyll-a (*chla*) as the reference parameter, the normalized correlation weight formula of the *j*-th parameter is as follows:

$$W_j = \frac{r_{ij}^2}{\sum_{j=1}^{m} r_{ij}^2} \quad (10)$$

where r_{ij} is the correlation coefficient between the *j*-th parameter and the reference parameter *chla* and *m* represents the number of evaluation parameters.

The correlation coefficients r_{ij} and r_{ij}^2 between *chla* and other parameters are shown in Table 2 (Li and Zhang, 1993).

Table 2

The correlation coefficients r_{ij} and r_{ij}^2 between *chla* and other parameters.

Parameter	TP	TN	SD	COD_{Mn}
r_{ij}	0.84	0.82	-0.83	0.83
r_{ij}^2	0.7056	0.6724	0.6889	0.6889

The calculation formula of the nutritional status index of each parameter is shown as follows:

$$TLI(TP) = 10(9.436 + 1.624 \ln TP) \quad (11)$$

$$TLI(TN) = 10(5.453 + 1.694 \ln TN) \quad (12)$$

$$TLI(SD) = 10(5.118 + 1.94 \ln SD) \quad (13)$$

$$TLI(COD_{Mn}) = 10(0.109 + 2.661 \ln COD_{Mn}) \quad (14)$$

where *TP* is total phosphorus; *TN* represents the total nitrogen; *SD* represents the Secchi depth, a measure of transparency; and COD_{Mn} is the chemical oxygen demand.

Among the parameters listed above, TP and TN are pivotal, and a limitation of TP or TN can limit algae blooms (Bennett et al., 2017; Morgenstern et al., 2015; Lewis et al., 2011). The nutrient status of the surface water in the Tangxi River tributary bay in different months was evaluated in this study according to the *TLI* (∑) method. The influence of water temperature was also considered during the nutrient status evaluation.

3 Results and discussion

3.1 Hydrological situation

The temporal variations in confluence flow and water level are shown in Fig. 6a. During July and from August to October, the flow value at the confluence was

289 negative, which indicated that the tributary bay was mainly affected by backwater
290 intrusions from the main reservoir. In contrast, the tributary bay was mainly affected
291 by backwater jacking from the main reservoir in other months (January - June and
292 November - December). The backwater intrusion weakened when the water level of
293 the main reservoir dropped, and it became obvious when the water level of the main
294 reservoir rose.

295 Periods of intrusions that occurred in other tributaries were investigated in
296 previous studies. Backwater intrusions were mainly concentrated in low water level
297 operation period and impoundment period in the Daning River (Zhao, 2017). The
298 water of the mainstream of TGR flowed backward into the Xiangxi Bay in the density
299 current at different plunging depths during the process of TGR impoundment at the
300 end of the flood season in autumn, and the intrusion was weak when the water level
301 fell (Ji et al., 2010; Yang et al., 2018). Compared to the results of previous studies, the
302 backwater intrusions showed obvious seasonal changes and the main intrusion time
303 was almost the same.

304 The temporal variation in confluence flow and the length of backwater are shown
305 in Fig. 6b. With the change in the flow at the confluence, the length of the backwater
306 also changed. During January to April and October to December, the water level of
307 the main reservoir was between 160 and 175 m and the backwater reached distances
308 of 39.8 - 42.6 km from the confluence simultaneously. During May to September, the
309 water level of the main reservoir remained at 145 - 160 m, and the backwater reached

distances of 12.6 - 23.8 km from the confluence.

The water level and the length of backwater had a negative correlation with the confluence flow. When the water level dropped, the value of the confluence flow was positive, and the length of backwater decreased. The tributary bay was mainly affected by the jacking of the main reservoir during this period. Conversely, when the water level rose, the water flow at the confluence was negative, and the length of the backwater increased. The tributary bay was mainly affected by backwater intrusions at this time.

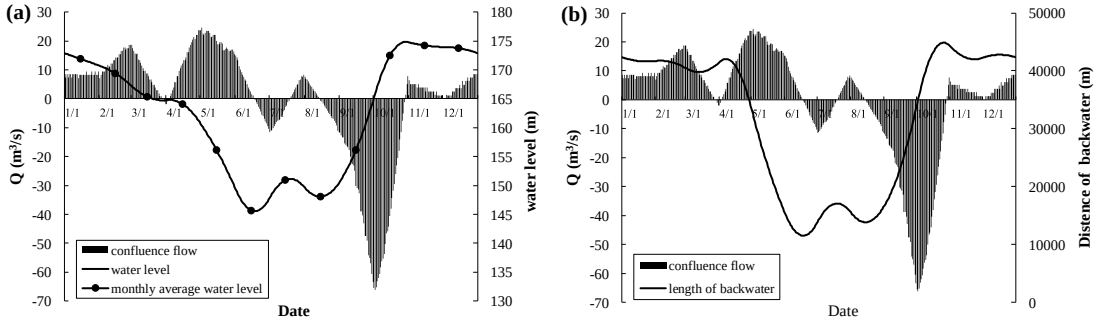

Fig. 6. Relationships among water level, length of backwater and confluence flow. (a) Daily variations in confluence flow and water level and (b) daily variations in confluence flow and length of backwater.

3.2 Hydrodynamics

The distribution of the flow field in each month is shown in Fig. 7. In each month, the upstream water flowed along the surface of the tributary bay or sank to the bottom. The backwater from the main reservoir entered the confluence at different depths simultaneously, forming one or two flow circulation patterns in the tributary bay. A similar flow field distribution occurred in other tributary bays of the TGR (Ji et al.,

2017).

In response to the jacking of the main reservoir in January, the water from the tail of the tributary bay first flowed along the surface and then sank to the bottom. Under the influence of geography, the backwater from the main reservoir formed two large counterclockwise circulations in the tributary bay. The water level gradually decreased from February to March, and the backwater effect of the main reservoir also gradually weakened. The water from the tail formed one circulation (February) or two circulations (March) in the tributary bay. From April to June, as the upstream water of the tributary bay joined the surface layer, the circulation zone disappeared. The upstream water gradually sank as it neared the confluence, and at the same time, the backwater from the main reservoir entered the tributary bay in the upper middle layers and formed a small counterclockwise circulation. From July to August, the upstream water of the tributary bay directly flowed to the confluence along the surface layer, and the backwater from the main reservoir entered the tributary bay in the middle and lower layers, forming one circulation in August and two circulations in July. In September, the upstream water first flowed through the surface layer and then sank to the middle of the tributary bay. The backwater from the main reservoir inclined upward from the lower layer and formed two circulations. The upper circulation was a smaller clockwise circulation, while the lower circulation was a larger counterclockwise circulation. The water level increased significantly from October to December, and the influence of the backwater increased simultaneously.

The upstream water of the tributary bay flowed through the surface layer and then sank to the bottom.

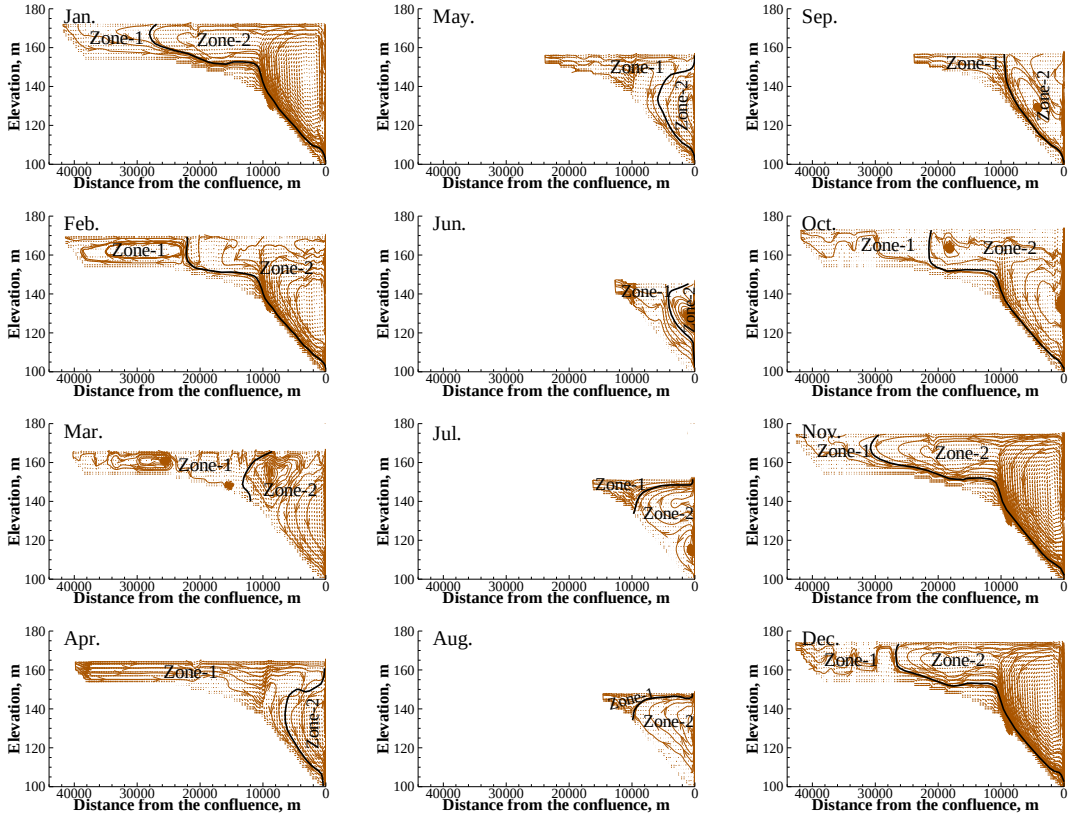

Fig. 7. Distribution of the flow field in each month. The flow field was divided into two areas (Zone 1 and Zone 2) according to the flow field characteristics. The black curve in the figure is the boundary between Zone 1 and Zone 2.

According to the distribution of the flow field, the tributary bay was divided into two different areas. Zone 1 represented the area mainly affected by the water from the tail of the tributary bay, and Zone 2 was the area mainly affected by the backwater from the main reservoir. Due to the variations in water level and flow value, the ranges of Zone 1 and Zone 2 differed in each month. The proportions of Zone 1 and Zone 2 varied with the water level and time (Fig. 8). From January to April, the

backwater reach was from the confluence to Jiangkou Town. With the decrease in the water levels, the proportion of Zone 1 increased, while the proportion of Zone 2 decreased. From May to September, the length of backwater decreased, and it only reached Nanxi Town. With the fluctuation in the water level in these months, the trend of the proportions of Zone 1 and Zone 2 became irregular. From October to November, with the rise in the water level, the proportion of Zone 1 decreased, while the proportion of Zone 2 increased. The opposite results were obtained from November to December when the water level gradually decreased. From October to December, the backwater again reached Jiangkou Town. These results suggested that the backwater had a greater impact on the tributary bay when the main reservoir was at a high water level and had a smaller impact when the main reservoir was at a low water level.

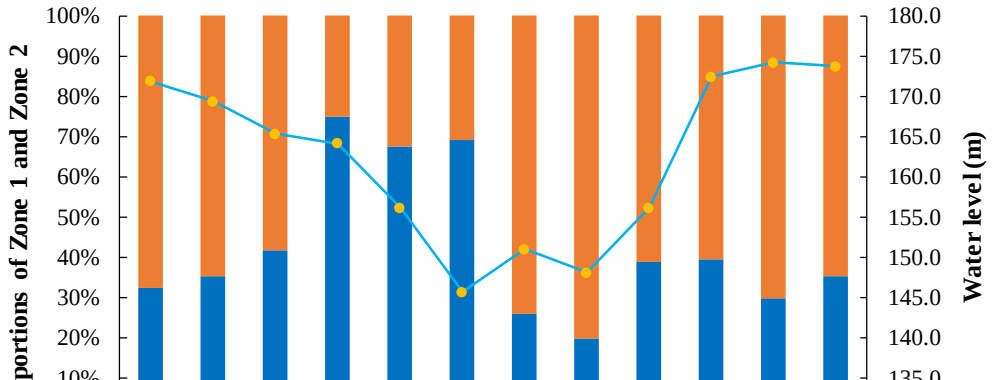

	Jan	Feb	Mar	Apr	May	Jun	Jul	Aug	Sep	Oct	Nov	Dec
Zone 2	68%	65%	58%	25%	33%	31%	74%	80%	61%	60%	70%	65%
Zone 1	32%	35%	42%	75%	67%	69%	26%	20%	39%	40%	30%	35%
water level	171.9	169.4	165.3	164.1	156.1	145.7	150.9	148.1	156.1	172.4	174.2	173.7

Fig. 8. Proportions of Zone 1 and Zone 2 and the variation in water level. The orange bar represents Zone 2, and the blue bar represents Zone 1. The blue dashed line represents the variation in water level.

3.3. Water temperature

Previous studies showed that the water temperature between the main reservoir and tributary bays were different, which led to the stratification of water temperature in the tributary bays (Ji et al., 2013). The water temperature distribution of the tributary bay in different months is shown in Fig. 9. From January to February, July to August, and October to December, the water temperatures in Zone 1 and Zone 2 were quite different. There was an obvious temperature boundary, which was mainly affected by the large difference between the upstream water temperature in the tributary bay and the backwater temperature from the main reservoir. From March to June and in September, the water temperature in Zone 1 was similar to that of Zone 2 due to the small difference between the water temperature at the tail of the tributary bay and the water temperature of the backwater from the main reservoir.

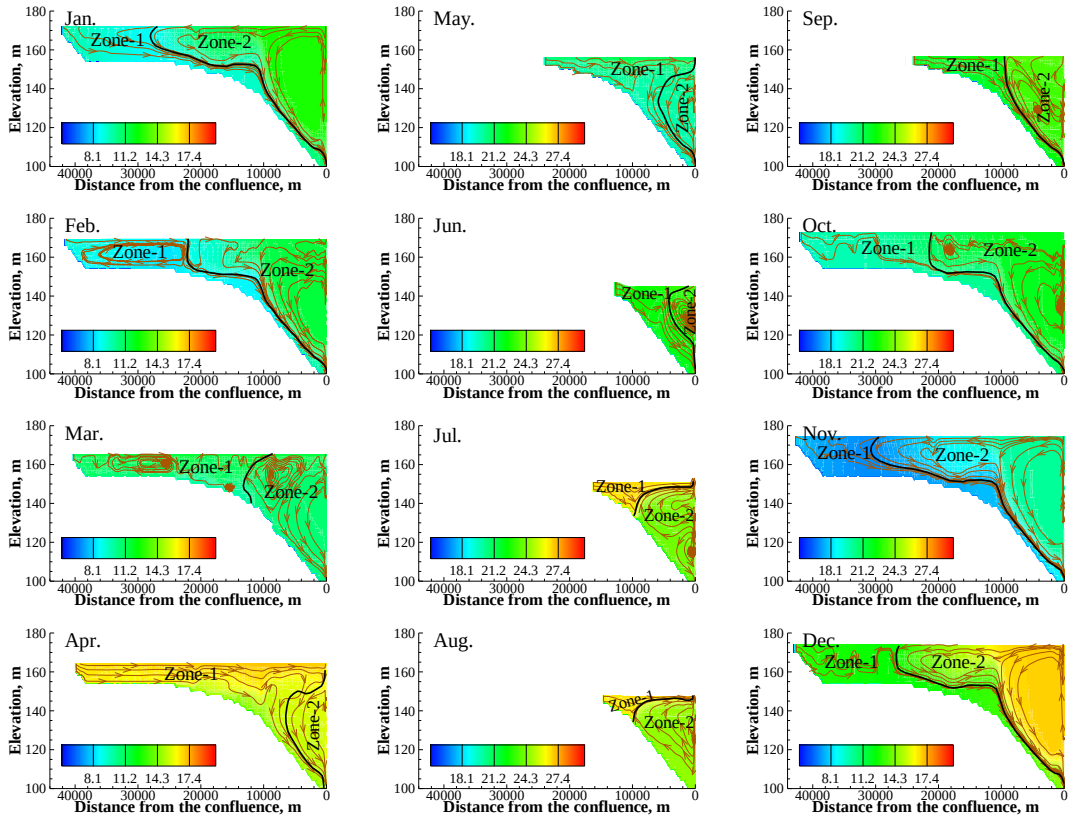

388

389 **Fig. 9.** Distribution of water temperature in different months. The black curve in the

390 figure is the boundary between Zone 1 and Zone 2. The brown curves with arrows are

391 streamlines.

392 The surface water temperatures of the tributary bay in each month are shown in

393 Fig. 10a. From March to June, due to the small difference between the upstream water

394 temperature of the tributary bay and the backwater temperature of the main reservoir,

395 the surface water temperature changed gently across the bay. The water temperature

396 gradually decreased from the confluence to the tail of the tributary bay from July to

397 August and gradually increased from September to October. The water temperature in

398 the middle reaches was slightly lower than the temperature at the confluence and the

399 tail of the tributary bay from January to February and from November to December.

The vertical water temperature in the confluence is shown in Fig. 10b. Affected by solar radiation and air temperature, the water temperature at the surface was relatively higher than that at the bottom (Zeng et al., 2016; Carey et al., 2012). The temperature in the middle layers changed little. There was a small thermocline in the surface water from May to August, and sinking of cold water occurred in January, February, and September to December.

The average water temperatures of Zone 1 and Zone 2 in different months are shown in Fig. 10c. The average water temperatures of Zone 1 and Zone 2 were similar from March to June and in September, while a difference of more than 1.5 ºC existed in other months. As the water of Zone 1 mainly came from the upstream of the tributary bay, it was significantly affected by the air temperature (Mohseni and Stefan, 1999). Zone 2 was mainly affected by the backwater from the main reservoir. Therefore, the average water temperature in Zone 1 was higher than that in Zone 2 in summer, and the average water temperature in Zone 1 was lower than that in Zone 2 in winter.

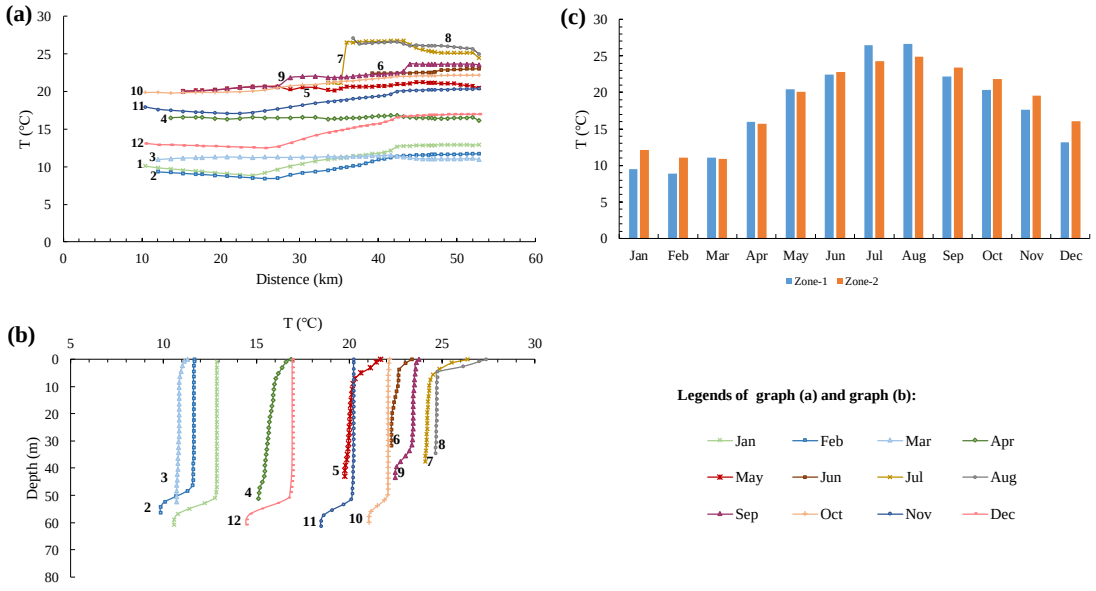

Fig. 10. Changes in water temperature. (a) Variation in surface water temperature in each month along the tributary bay; (b) Variation in the vertical water temperature at the confluence in each month. (c) Average water temperatures of Zone 1 and Zone 2 in each month. The blue bar represents Zone 1, and the orange bar represents Zone 2 in panel (c).

3.4 Water quality

The water exchange between the main reservoir and tributary bay was an important factor driving the variation of water quality distribution and nutrient structure in the tributary bay (Zhao et al., 2015; Han et al., 2020). As shown in Fig. 11, the COD concentration in the tributary bay ranged from 0 - 13 mg/L. There was no significant difference in COD concentrations between the tail of the tributary bay and the backwater from the main reservoir, both of which had values between 8 and 11 mg/L. With a decreasing trend along the bay, the concentration of COD reached a minimum value at the intersection of Zone 1 and Zone 2.

The NH_3-N concentration in the tributary bay was in the range of 0 - 0.3 mg/L (Fig. 12). Since the concentration of NH_3-N in the tail of the tributary bay was higher than that of the backwater from the main reservoir, the concentration of NH_3-N in Zone 1 was higher than that in Zone 2 from January to March and July to December. There was no significant difference in NH_3-N between the tail of the tributary bay and the backwater from the main reservoir in April to June. Additionally, with a decreasing trend along the bay, the concentration of NH_3-N was lower at the intersection of Zones 1 and 2 than at the tail of the tributary bay or the confluence.

The distributions of TP and TN proved that the nutrients in tributary bays did not originate solely in the tributary bays but instead were mainly from the main reservoir, and they also showed that the nutrient levels were different across seasons. The distributions of TP and TN in the tributary bay were almost the same. The concentration near the confluence was relatively high. With the mixing of the water from the tail of the tributary bay and the backwater from the main reservoir and with the degradation of water quality, the concentrations of TP and TN gradually decreased. In particular, the concentration of TP was in the range of 0.04 - 0.12 mg/L, and the concentration of TN was in the range of 0.8 - 2.1 mg/L. The concentrations of TP and TN in Zone 2 were higher than those in Zone 1. There was an obvious quality concentration boundary in the tributary bay, which was basically consistent with the regional boundary of the flow field. Furthermore, there was an obvious transition zone near the quality boundary in January to May and September to December, while the

transition zone in June to August was very weak.

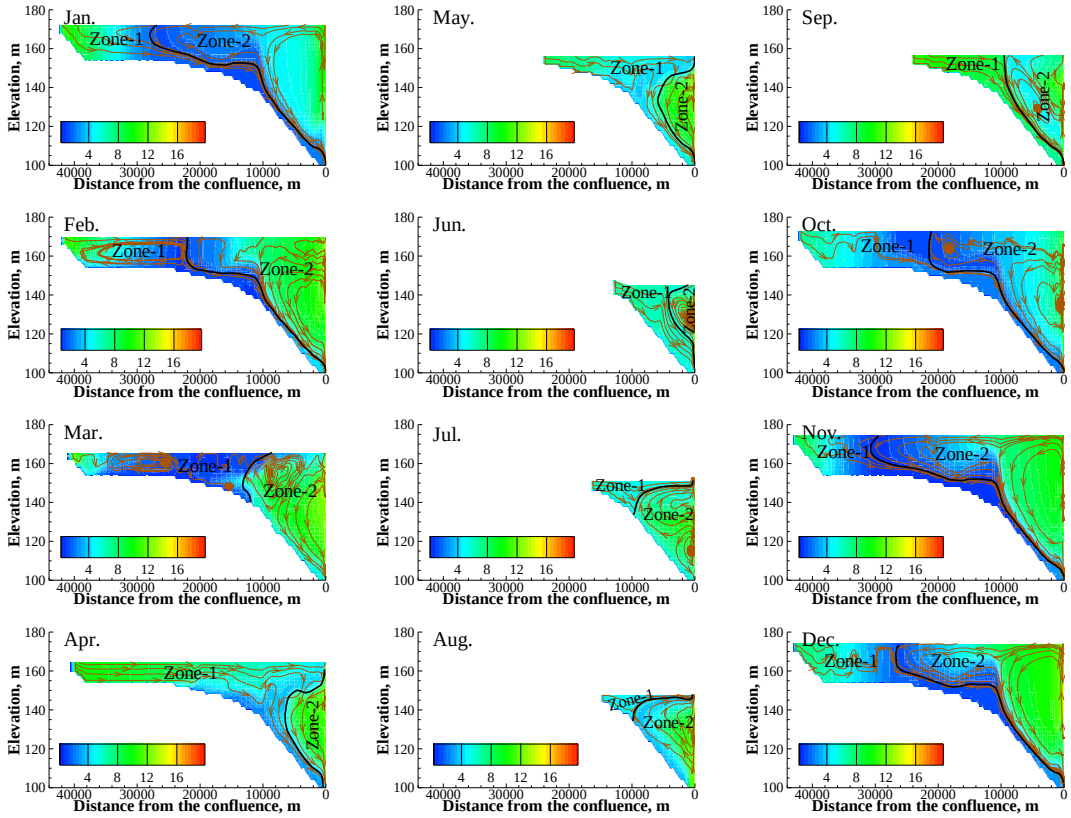

Fig. 11. Distribution of COD in each month. The black curve in the figure is the boundary between Zone 1 and Zone 2. The brown curves with arrows are streamlines.

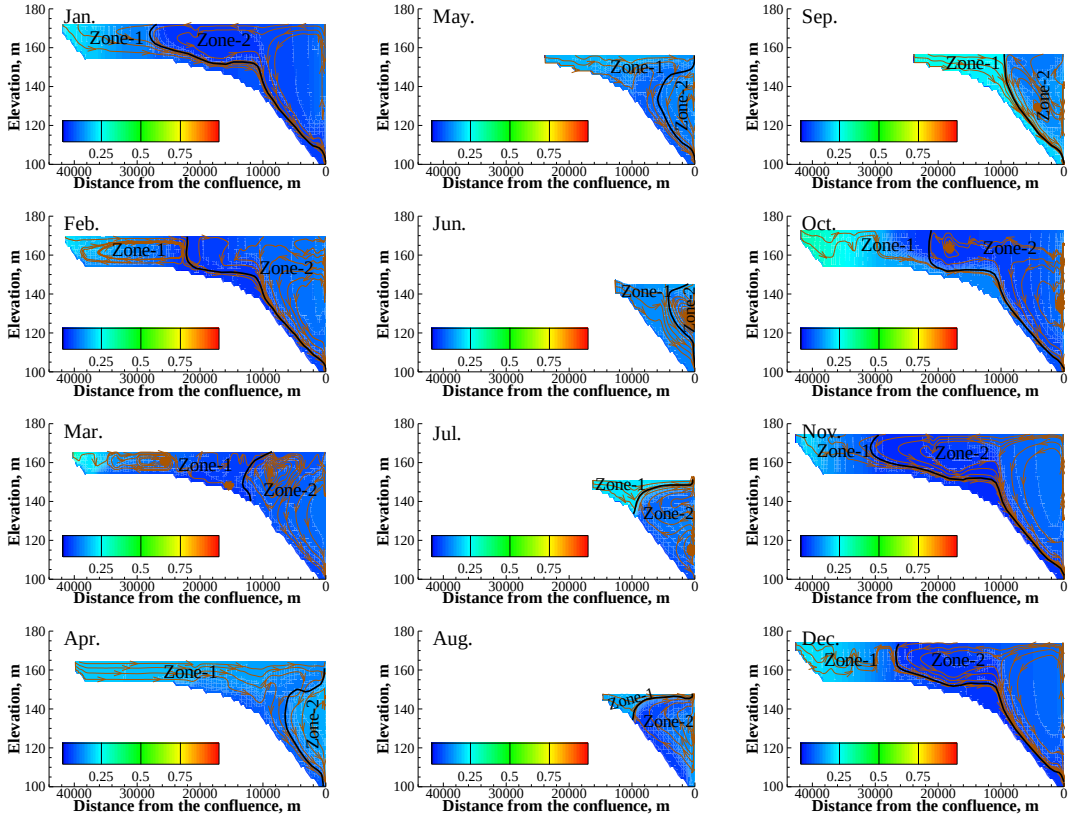

Fig. 12. Distribution of NH_3-N in each month. The black curve in the figure is the boundary between Zone 1 and Zone 2. The brown curves with arrows are streamlines.

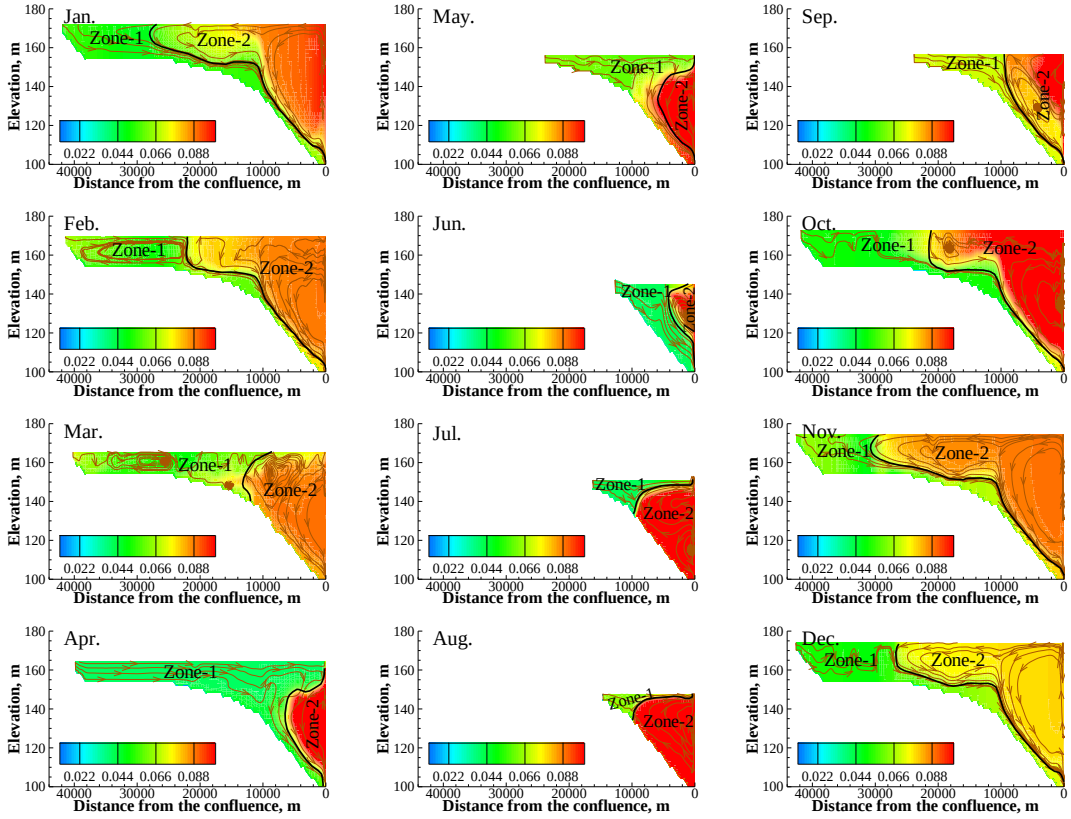

458

459 **Fig. 13.** Distribution of TP in each month. The black curve in the figure is the

460 boundary between Zone 1 and Zone 2. The brown curves with arrows are streamlines.

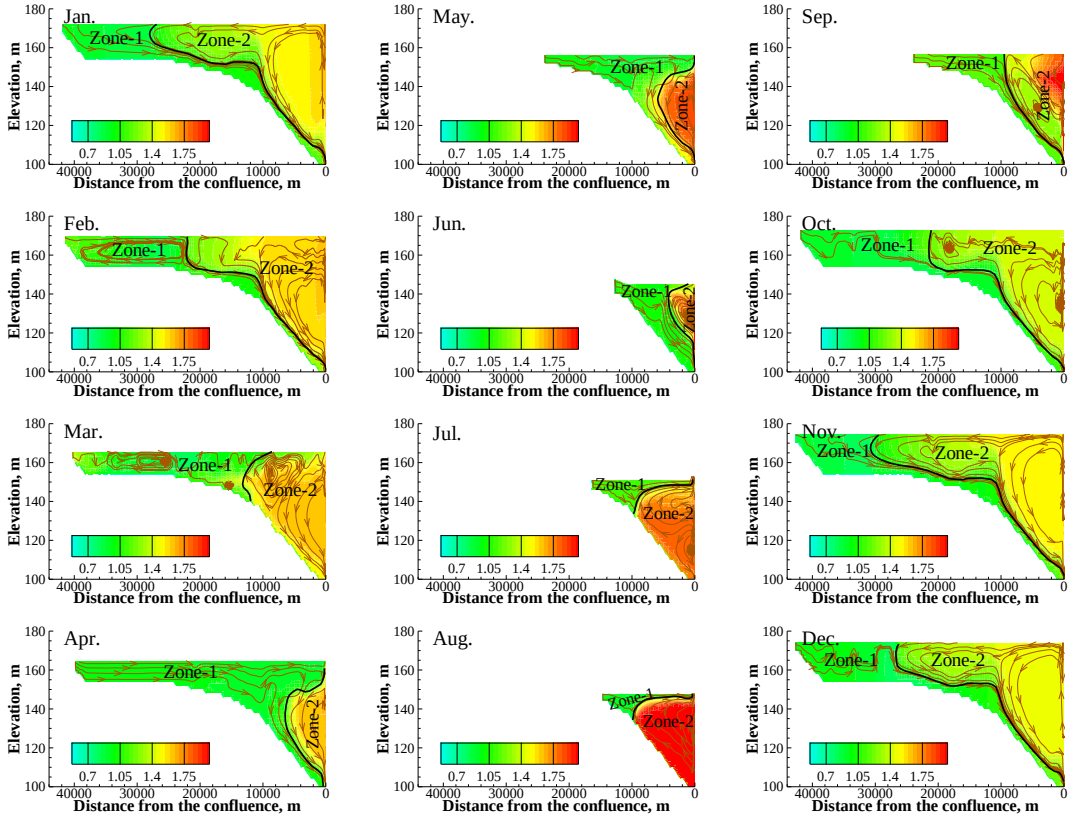

Fig. 14. Distribution of TN in each month. The black curve in the figure is the boundary between Zone 1 and Zone 2. The brown curves with arrows are streamlines.

The COD, NH_3-N, TP and TN in the surface water of the tributary bay in different months are shown in Fig. 15. The concentrations of COD and NH_3-N were generally higher on the two sides and lower in the middle. The concentrations of TP and TN were higher in the confluence and lower in the tail of the tributary bay.

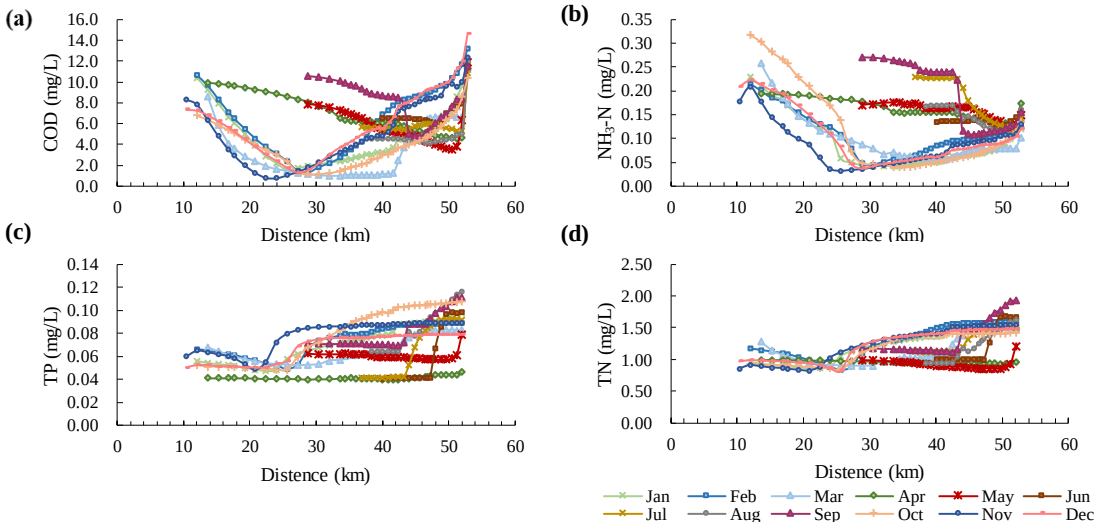

468

469 **Fig. 15.** Variation in surface water quality in different months along the tributary bay.
470 (a) Variation in chemical oxygen demand; (b) Variation in ammonia nitrogen, (c)
471 Variation in total phosphorus; (d) Variation in total nitrogen.

472 The vertical changes in COD, NH_3-N, TP and TN in different months at the
473 confluence are shown in Fig. 16. There was no obvious regularity in the vertical water
474 quality distributions of COD and NH_3-N. The average vertical variation in COD was
475 4.6 mg/L over 12 months. The largest change appeared in December, with a value of
476 7.0 mg/L, and the smallest change appeared in June, with a value of 1.6 mg/L. The
477 average vertical variation in NH_3-N was 0.06 mg/L. The largest change appeared in
478 January, with a value of 0.02 mg/L, and the smallest change appeared in July, with a
479 value of 0.12 mg/L.

480 The concentrations of TP and TN were higher in the surface water and lower in
481 the bottom in January to March and September to December, which was contrary to
482 that in July and August. From April to June, the concentrations of TP and TN first

increased and then decreased from the surface to the bottom. The concentration gradient in the upper 10 m surface layer was relatively large.

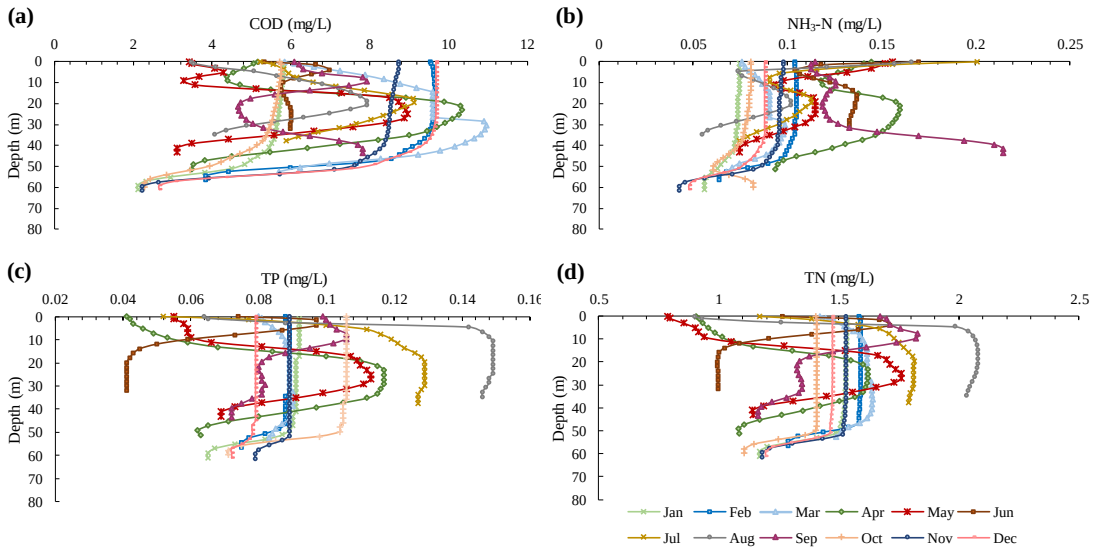

Fig. 16. Vertical variation in the water quality in different months at the section that was 6 km away from the confluence. (a) Variation in chemical oxygen demand; (b) Variation in ammonia nitrogen; (c) Variation in total phosphorus; (d) Variation in total nitrogen.

The average concentrations of COD, NH_3-N, TP and TN in Zone 1 and Zone 2 are shown in Fig. 17. The COD concentration in Zone 2 was higher than that in Zone 1 in all months except September. The concentration of NH_3-N in Zone 1 was generally higher than that in Zone 2 due to the higher concentration of NH_3-N in the water from the tail of the tributary bay. For TP and TN, the concentrations in Zone 2 were higher than those in Zone 1.

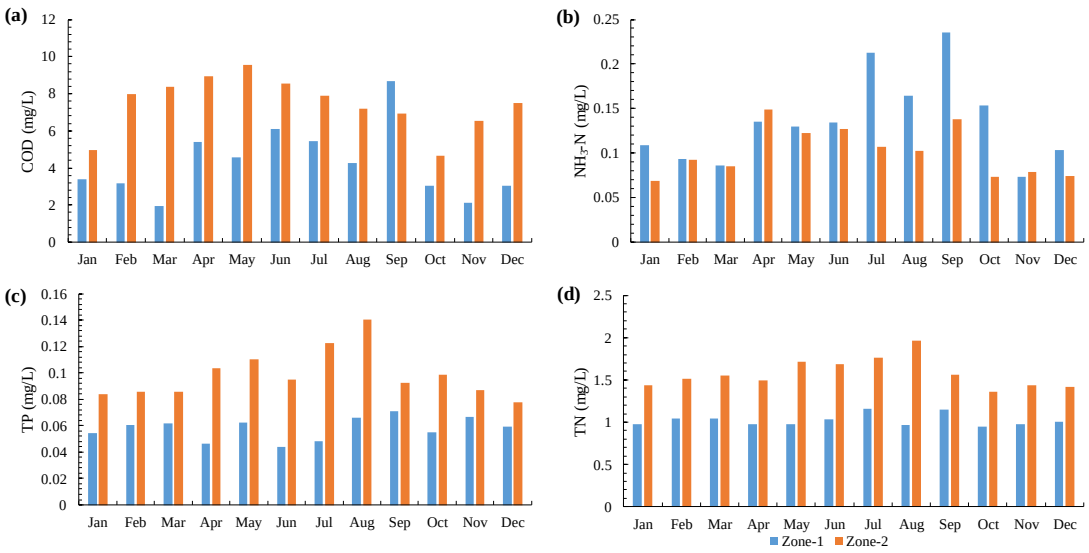

Fig. 17. Average water quality changes in Zone 1 and Zone 2. (a) Variation in chemical oxygen demand; (b) Variation in ammonia nitrogen; (c) Variation in total phosphorus; (d) Variation in total nitrogen. The blue bar represents Zone 1, and the orange bar represents Zone 2.

3.5 Water eutrophication

The distribution of the *TLI* (∑) values in the surface water of the tributary bay in different months is shown in Fig. 18. The *TLI* (∑) within 0.5 km of the confluence was relatively higher than in other areas throughout the year, reaching the level of light eutrophication. Additionally, the reach with high *TLI* (∑) values in February and in September to December had a long range. From January to March and September to December, the reach approximately 25 km from the confluence had low *TLI* (∑) values, reaching oligotrophic status. In the rest of the time and area, the *TLI* (∑) values correspond to a medium nutrient level. Additionally, the water temperature near the confluence was less than 20 ºC, and the light conditions were poor in January

511 to April and November to December. Temperature and light conditions are important
512 factors in the occurrence of eutrophication, and neither low temperatures nor poor
513 light conditions are conducive to the growth of algae (Singh and Singh, 2015;
514 Romarheim et al., 2015; Paerl et al., 2011; Reynolds, 2006). Physical dynamics play a
515 critical role in estuarine biological production, material transport and water quality
516 (Kasai et al., 2010). The results of this study showed that the tributary bay was mainly
517 affected by backwater intrusions from the main reservoir in July and from August to
518 October. During this time, the vertical mixing of water near the confluence was severe,
519 which was also not conducive to the growth of algae (Gao et al., 2017; Lindim et al.,
520 2011; Huisman et al., 2006). In conclusion, considering the influence of
521 hydrodynamics, water temperature and water quality, the risk of eutrophication in the
522 tributary bay was highest in the section within 0.5 km of the confluence from May to
523 June. Wu et al (2010) constantly monitored the eutrophication of the Daning River, a
524 tributary bay of the TGR, and found that algal blooms frequently occurred in the area
525 close to the confluence from March to June, which was similar to the results of the
526 present study.

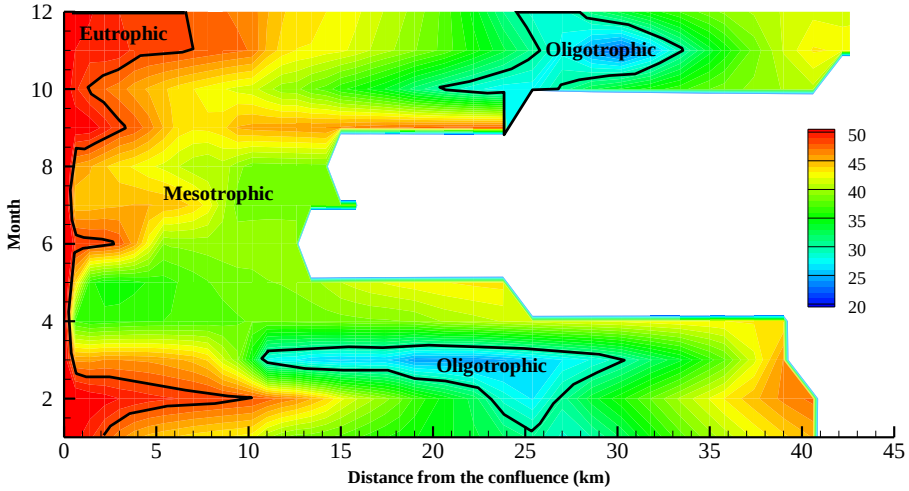

Fig. 18. Eutrophication results of surface water in the tributary bay. The nutrient status of the tributary bay is divided into three states (oligotrophic, mesotrophic and eutrophic) according to the comprehensive nutrient index.

3.6 Sensitivity of the results to the model forcing factors

The link between the main reservoir and its tributary bay is the hydrodynamic condition, and it is mostly affected by water level fluctuations (Sha et al., 2015). Thus, in previous chapters, we mainly discussed the effect of water level fluctuations in detail. Air temperature and winds conditions were also important factors affecting the results (Yu et al., 2013; Huang et al., 2016). Air temperature can affect the surface water temperature by promoting the formation of thermal stratification (Jin et al., 2019). From July to August, air temperature was a dominant variable and the stratification of water temperature was obvious. A comparison of the distributions of the water temperature and water quality showed that air temperature had almost no effect on the water quality distribution, while the water level fluctuation was a

542 determining factor. The results were not sensitive to wind conditions because the wind
543 varied little throughout the year and the wind speed was small (1 - 1.8 m/s) in the
544 study area.

545 **4 Conclusions and future work**

546 In this paper, the effect of the backwater jacking and intrusions from the main
547 reservoir on the hydrodynamics and water environment of the Tangxi River, a
548 tributary bay of the TGR are studied. The following conclusions were reached as a
549 result of this research:

550 (1) The intrusion was weak when the water level of the main reservoir dropped,
551 and the tributary bay was mainly affected by the backwater jacking of the main
552 reservoir. The periods of intrusions in the tributary bay ranged from July to October.
553 Conversely, when the water level of the main reservoir rose, the tributary bay was
554 mainly affected by backwater intrusions from the main reservoir.

555 (2) The water from the tail flowed along the surface of the tributary bay or sank to
556 the bottom in each month. The backwater from the main reservoir entered the
557 confluence at different depths simultaneously, forming one or two circulations in the
558 tributary bay. The backwater had a greater impact on the tributary bay when the main
559 reservoir was at high water level and had a smaller impact when the main reservoir
560 was at a low water level.

561 (3) The water temperature of the tributary bay was not greatly affected by the
562 backwater from the main reservoir. The concentrations of COD and NH_3-N in the

563 tributary bay were generally higher at the two ends of the bay and lower in the middle.
564 For TP and TN, there was an obvious quality concentration boundary in the tributary
565 bay, which was basically consistent with the regional boundary of the flow field. The
566 concentrations of TP and TN were higher at the side near the confluence.

567 (4) Nutrients in tributary bays were mainly from the main reservoir and the
568 nutrient levels were affected by the constantly changing hydrodynamic conditions and
569 environmental factors across seasons. The risk of eutrophication of the tributary bay
570 was high within 0.5 km of the confluence in May and June.

571 This paper only studied the influence of the main reservoir on the tributary bay in
572 terms of hydrodynamics and water environment. The operations of the main reservoir
573 may have common influences on the tributary bays, and tributary bays may also
574 influence the main reservoir. The influence of the tributary bay on the main reservoir
575 and the interaction between the main reservoir and the tributary bay are still unclear.
576 In the future, numerical simulation of the main reservoir’s hydrodynamics and water
577 environment based on the results of this paper should be carried out to explore the
578 interaction between the main reservoir and the tributary bay.

579 Future work should also explore control measures to improve the water
580 environment of the tributary bay based on its interaction with the main reservoir. At
581 present, some scholars have proposed that preventing and controlling eutrophication
582 in tributary bays can be achieved by the method of "double nutrient reduction", which
583 involves the simultaneous control of the nutrient inputs from the main stream and the

584 tributary (Liang et al., 2014). It is also possible to use ecological methods, such as
585 emergent plants, submerged plants, phytoplankton, benthic organisms and fish, to
586 improve water eutrophication (Srivastava et al., 2017; Li et al., 2013; Soares et al.,
587 2011). In addition, the concept of improving the hydrodynamic conditions of the main
588 stream and controlling the eutrophication of the water body through manually
589 controlled operation has been widely accepted by many experts and scholars (Yao,
590 2011; Zheng et al., 2011; Naselli-Flores and Barone, 2005). Based on future research
591 on the interaction between the main reservoir and the tributary bay with the goal of
592 ensuring the main function of the main reservoir, water environment protection
593 measures should be reasonably proposed for tributary bays in the future.

594 *Declaration of Competing Interest.* We declare that we have no known competing
595 financial interests or personal relationships that could have appeared to influence the
596 work reported in this paper.

597 *Acknowledgements.* This work was sponsored by the fund of Sichuan Province under
598 permission number 2018SZYZF0001.

599 *Author contribution.* All co-authors participated in the field collection, data analysis,
600 and/or writing of this manuscript. Ruifeng Liang was primarily responsible for
601 preparation and process of this manuscript. Xintong Li and Yuanming Wang
602 conceived of the study design and data analysis with input from all co-authors.

603 **References**

604 Bennett, M. G., Schofield, K. A., Lee, S. S. and Norton, S. B.: Response of

chlorophyll a to total nitrogen and total phosphorus concentrations in lotic ecosystems: a systematic review protocol, Environmental Evidence, 6(1), 18, https://doi.org/10.1186/s13750-017-0097-8, 2017.

Berger, C. J., and Wells, S. A.: Modeling the effects of macrophytes on hydrodynamics. Journal of Environmental Engineering, 134(9), 778-788, https://doi.org/10.1061/(ASCE)07339372(2008)134:9(778), 2008.

Bockelmann, B. N., Fenrich, E. K., Lin, B. and Falconer, R. A.: Development of an ecohydraulics model for stream and river restoration, Ecological Engineering, 22(4-5), 227-235, https://doi.org/10.1016/j.ecoleng.2004.04.003, 2004.

Bowen, J. D., and Hieronymus, J. W.: A CE-QUAL-W2 model of Neuse Estuary for total maximum daily load development, Journal of Water Resources Planning and Management, 129(4), 283-294, https://doi.org/10.1061/(ASCE)0733-9496(2003)129:4(283), 2003.

Cai, Q. and Hu, Z.: Studies on eutrophication problem and control strategy in the Three Gorges Reservoir, Acta Hydrobiologica Sinica, 30(1), 7-11 (in Chinese), https://doi.org/10.3321/j.issn:1000-3207.2006.01.002, 2006.

Carey, C. C., Ibelings, B. W., Hoffmann, E. P., Hamilton, D. P. and Brookes, J. D.: Eco-physiological adaptations that favour freshwater cyanobacteria in a changing climate, Water Research, 46(5), 1394-1407, https://doi.org/10.1016/j.watres.2011.12.016, 2012.

Carlson, R. E.: A trophic state index for lakes. Limnology and Oceanography, 22(2),

361-369, https://doi.org/10.4319/lo.1977.22.2.0361, 1977.

Debele, B., Srinivasan, R. and Parlange, J. Y.: Coupling upland watershed and downstream waterbody hydrodynamic and water quality models (SWAT and CE-QUAL-W2) for better water resources management in complex river basins, Environmental Modeling & Assessment, 13(1), 135-153, https://doi.org/10.1007/s10666-006-9075-1, 2008.

Deng, S. and Bai, Y.: Analysis on the role of environmental impact assessment in the construction of water conservancy and hydropower projects, Environment and Sustainable Development, 41(5), 101-102 (in Chinese), https://doi.org/10.19758/j.cnki.issn1673-288x.2016.05.030, 2016.

Fang, J.: The Operating Simulation of Cascade Reservoirs and it's Impacts on River Eco-environment—A Case Study on Upper reaches of the Yangtze River. Ph.D, Institute of Mountain Hazards and Environment Chinese Academy of Sciences, 2007.

Feng, J., Li, R., Liang, R. and Shen, X.: Eco-environmentally friendly operational regulation: an effective strategy to diminish the TDG supersaturation of reservoirs, Hydrology and Earth System Sciences, 18, 1213-1223, https://doi.org/10.5194/hess-18-1213-2014, 2014.

Fu, B., Wu, B., Lu, Y., Xu, Z., Cao, J., Niu, D., Yang, G., and Zhou, Y.: Three gorges project: efforts and challenges for the environment, Progress in Physical Geography, 34(6), 741-754, https://doi.org/10.1177/0309133310370286, 2010.

647 Gao, Q., He, G., Fang, H. and Huang, L.: Effects of vertical mixing on algal growth in
648 the tributary of Three Gorges Reservoir, Journal of Hydraulic Engineering 48(1),
649 96-103 (in Chinese), https://doi.org/10.13243/j.cnki.slxb.20160239, 2017.
650 Gao, X., Zeng, Y., Wang, J. and Liu, H.: Immediate impacts of the second
651 impoundment on fish communities in the Three Gorges Reservoir, Environmental
652 Biology of Fishes, 87, 163-173, https://doi.org/10.1007/s10641-009-9577-1, 2010.
653 Han, C., Qin, Y., Ma, Y., Zhao, Y., Liu, Z., Yang, C., and Zhang, L.: Cause of
654 Variation in Water Quality Distribution and Its Ecological Effects in the Daning
655 Bay of the Three Gorges Reservoir, Research of Environmental Sciences, 33(4),
656 893-900 (in Chinese), https://doi.org/10.13198/j.issn.1001-6929.2019.09.03, 2020.
657 Holbach, A., Bi, Y., Yuan, Y., Wang, L., Zheng, B. and Norra, S.: Environmental water
658 body characteristics in a major tributary backwater of the unique and strongly
659 seasonal Three Gorges Reservoir, China, Environmental Science Processes:
660 Processes & Impacts, 17(9), 1641-1653, https://doi.org/10.1039/C5EM00201J,
661 2015.
662 Holbach, A., Norra, S., Wang, L. Yuan, Y., Wei, H. and Zheng, B.: Three Gorges
663 Reservoir: Density Pump Amplification of Pollutant Transport into Tributaries,
664 Environmental Science & Technology, 48(14), 7798-7806,
665 https://doi.org/10.1021/es501132k, 2014.
666 Hu, B., Yang, Z., Wang, H., Sun, X., Bi, N. and Li, G.: Sedimentation in the Three
667 Gorges Dam and the future trend of Changjiang (Yangtze River) sediment flux to

668 the sea, Hydrology and Earth System Sciences, 13, 2253-2264,
669 https://doi.org/10.5194/hess-13-2253-2009, 2009.
670 Huisman, J., Pham Thi, N. N., Karl, D. M. and Sommeijer, B.: Reduced mixing
671 generates oscillations and chaos in the oceanic deep chlorophyll maximum,
672 Nature, 439(7074), 322-325, https://doi.org/10.1038/nature04245, 2006.
673 Hu, N., Ji, D., Liu, D., Huang, Y., Yin, W., Xiong, C., and Zhang, Y.: Field monitoring
674 and numerical simulating on three-dimensional thermal density currents in the
675 estuary of xiangxi river, Applied Mechanics & Materials, 295-298, 1029-1036,
676 https://doi.org/10.4028/www.scientific.net/AMM.295-298.1029, 2013.
677 Huang, L., Fang, H., He, G., Jiang, H. and Wang, C.: Effects of internal loading on
678 phosphorus distribution in the Taihu Lake driven by wind waves and lake currents,
679 Environmental Pollution, 219, 760-773,
680 https://doi.org/10.1016/j.envpol.2016.07.049, 2016.
681 Ji, D., Liu, D., Yang, Z. and Xiao, S.: Hydrodynamic characteristics of Xiangxi Bay in
682 Three Gorges Reservoir, Science China (Physics, Mechanics & Astronomy), 40(1),
683 101-112 (in Chinese), https://doi.org/CNKI:SUN:JGXK.0.2010-01-013, 2010.
684 Ji, D., Huang, Y., Liu, D., Yin, W., Yang, Z., Ma, J., and Xie, T.: Research progress on
685 the ocean estuary and its enlightenment to the study of the tributary in Three
686 Gorges Reservoir, Applied Mechanics and Materials, 295, 2215-2222,
687 https://doi.org/10.4028/www.scientific.net/AMM.295-298.2215, 2013.
688 Ji, D., Wells, S. A., Yang, Z., Liu, D., Huang, Y., Ma, J. and Chris, J. B.: Impacts of

689 water level rise on algal bloom prevention in the tributary of Three Gorges
690 Reservoir, China, Ecological Engineering, 98, 70-81,
691 https://doi.org/10.1016/j.ecoleng.2016.10.019, 2017.
692 Kasai, A., Kurikawa, Y., Ueno, M., Robert, D., and Yamashita, Y.: Salt-wedge
693 intrusion of seawater and its implication for phytoplankton dynamics in the Yura
694 Estuary, Japan, Estuarine, Coastal and Shelf Science, 86(3), 408-414,
695 https://doi.org/10.1016/j.ecss.2009.06.001, 2010.
696 Lewis, W. M., Wurtsbaugh, W. A. and Paerl, H. W.: Rationale for control of
697 anthropogenic nitrogen and phosphorus to reduce eutrophication of inland waters,
698 Environmental Science & Technology, 45(24), 10300-10305,
699 https://doi.org/10.1021/es202401p, 2011.
700 Li, K., He, W., Hu, Q. and Gao, S.: Ecological restoration of reclaimed wastewater
701 lakes using submerged plants and zooplankton, Water and Environment Journal,
702 28(3), 323-328, https://doi.org/10.1111/wej.12038, 2013.
703 Li, Z. and Zhang, H.: Trophic State Index and its Correlation with Lake Parameters in
704 China, Acta Scientiae Circumstantiae, 13(4), 391-397 (in Chinese),
705 https://doi.org/10.13671/j.hjkxxb.1993.04.002, 1993.
706 Liang, L., Deng, Y., Zheng, M. and Wei, X.: Predicting of Eutrophication in the
707 Longchuan River Based on CE-QUAL-W2 Model, Resources and Environment in
708 the Yangtze Basin, 23(1), 103-111, https://doi.org/10.11870/cjlyzyyhj2014Z1015,
709 2014.

Lindim, C., Pinho, J. L. and Vieira, J. M. P.: Analysis of spatial and temporal patterns in a large reservoir using water quality and hydrodynamic modeling, Ecological Modelling, 222(14), 2485-2494, https://doi.org/10.1016/j.ecolmodel.2010.07.019, 2011.

Liu, D., Yang, Z., Ji, D., Ma, J. and Cui, Y.: A review on the mechanism and its controlling methods of the algal blooms in the tributaries of Three Gorges Reservoir, Journal of Hydraulic Engineering, 47(03), 443-454 (in Chinese), https://doi.org/10.13243/j.cnki.slxb.20151304, 2016.

Liu, L.: Effects of vertical mixing on phytoplankton blooms in Xiangxi Bay of Three Gorges Reservoir: Implications for management, Water Research, 46(07), 2121-2130, https://doi.org/10.1016/j.watres.2012.01.029, 2012.

Long, L., Ji, D., Yang, Z., Ma, J., Scott, A. W., Liu, D. and Andreas, L.: Density - driven water circulation in a typical tributary of the Three Gorges Reservoir, China, River Research and Application, 35(7), 1-11, https://doi.org/10.1002/rra.3459, 2019.

Long, L., Xu H., Bao, Z., Ji, D. and Liu, D.: Temporal and spatial characteristics of water temperature in Xiluodu Reservoir, Journal of Hydroelectric Engineering, 37(4), 79-89 (in Chinese), https://doi.org/10.11660/slfdxb.20180408, 2018.

Lu, Q., Li, R., Li, J., Li, K. and Wang, L.: Experimental study on total dissolved gas supersaturation in water, Water Science and Engineering, 04(4), 396-404, https://doi.org/10.3882/j.issn.1674-2370.2011.04.004, 2011.

731 Lung, W. S., and Nice, A. J.: Eutrophication model for the Patuxent estuary: Advances
732 in predictive capabilities, Journal of Environmental Engineering, 133(9), 917-930,
733 https://doi.org/10.1061/(ASCE)0733-9372(2007)133:9(917), 2007.
734 McGrath, K. E., Dawley, E. M. and Geist, D. R.: Total Dissolved Gas Effects on
735 Fishes of the Lower Columbia River, PNNL-15525, Pacific Northwest National
736 Laboratory, Richland, Washington, https://doi.org/10.2172/918864, 2006.
737 Mohseni, O. and Stefan, H. G.: Stream temperature/air temperature relationship: a
738 physical interpretation, Journal of Hydrology, 218(3), 128-141,
739 https://doi.org/10.1016/S0022-1694(99)00034-7, 1999.
740 Morgenstern, U., Daughney, C. J., Leonard, G., Gordon, D., Donath, F. M., and
741 Reeves, R.: Using groundwater age and hydrochemistry to understand sources and
742 dynamics of nutrient contamination through the catchment into Lake Rotorua,
743 New Zealand, Hydrology and Earth System Sciences, 19, 803-822,
744 https://doi.org/10.5194/hess-19-803-2015, 2015.
745 Naselli-Flores, L. and Barone, R.: Water-Level Fluctuations in Mediterranean
746 Reservoirs: Setting a Dewatering Threshold as a Management Tool to Improve
747 Water Quality, Hydrobiologia, 548, 85-99,
748 https://doi.org/10.1007/s10750-005-1149-6, 2005.
749 Noori, R., Yeh, H. D., Ashrafi, K., Rezazadeh, N., Bateni, S. M., Karbassi, A.,
750 Kachoosangi, F. T. and Moazami, S.: A reduced-order based CE-QUAL-W2
751 model for simulation of nitrate concentration in dam reservoirs, Journal of

752 Hydrology, 530, 645-656, https://doi.org/10.1016/j.jhydrol.2015.10.022, 2015.
753 Oldani, N. O. and Claudio R. M. Baigún: Performance of a fishway system in a major
754 South American dam on the Parana River (Argentina–Paraguay), River Research
755 and Application, 18(2), 171-183, https://doi.org/10.1002/rra.640, 2002.
756 Paerl, H. W., Hall, N. S. and Calandrino, E. S.: Controlling harmful cyanobacterial
757 blooms in a world experiencing anthropogenic and climatic-induced change,
758 Science of the Total Environment, 409(10), 1739-1745,
759 https://doi.org/10.1016/j.scitotenv.2011.02.001, 2011.
760 Pan, X., Tang, L., Feng, J., Liang, R., Pu, X., Li, R., and Li, K.: Experimental
761 Research on the Degradation Coefficient of Ammonia Nitrogen Under Different
762 Hydrodynamic Conditions, Bulletin of Environmental Contamination and
763 Toxicology, 104, 288, https://doi.org/10.1007/s00128-019-02781-0, 2020.
764 Peng, C., Chen, L., Bi, Y., Xia, C., Lei, Y., Yang, Y., Jian, T. and Hu, Z.: Effects of
765 flood regulation on phytoplankton community structure in the Xiangxi River, a
766 tributary of the Three Gorges Reservoir, China Environmental Science, 34,
767 1863-1871, https://doi.org/10.1097/NEN.0000000000000183, 2014.
768 Ran, X., Alexander, F. B., Yu, Z. and Liu, J.: Implications of eutrophication for
769 biogeochemical processes in the Three Gorges Reservoir, China, Regional
770 Environmental Change, 19(1), 55-63, https://doi.org/10.1007/s10113-018-1382-y,
771 2019.
772 Reynolds, C. S.: The ecology of phytoplankton, Cambridge University Press, London,

2006.

Romarheim, A. T., Tominaga, K., Riise, G., and Andersen, T.: The importance of year-to-year variation in meteorological and runoff forcing for water quality of a temperate, dimictic lake, Hydrology and Earth System Sciences, 19, 2649-2662, https://doi.org/10.5194/hess-19-2649-2015, 2015.

Sha, Y., Wei, Y., Li, W., Fan, J. and Cheng, C.: Artificial tide generation and its effects on the water environment in the backwater of Three Gorges Reservoir, Journal of Hydrology, 528, 230-237, https://doi.org/10.1016/j.jhydrol.2015.06.020, 2015.

Singh, S. P. and Singh, P.: Effect of temperature and light on the growth of algae species: A review, Renewable and Sustainable Energy Reviews, 50, 431-444, https://doi.org/10.1016/j.rser.2015.05.024, 2015.

Soares, M., Vale, M. and Vasconcelos, V.: Effects of nitrate reduction on the eutrophication of an urban man-made lake (Palácio de Cristal, Porto, Portugal), Environmental Technology, 32(9), 1009-1015, https://doi.org/10.1080/09593330.2010.523437, 2011.

Srivastava, A., Chun, S. J., Ko, S. R., Kim, J., Ahn, C. Y. and Oh, H-M.: Floating rice-culture system for nutrient remediation and feed production in a eutrophic lake, Journal of Environmental Management, 203, 342-348, https://doi.org/10.1016/j.jenvman.2017.08.006, 2017.

Tang, Q., Bao, Y., He, X., Fu, B., Adrian, L. C. and Zhang, X.: Flow regulation manipulates contemporary seasonal sedimentary dynamics in the reservoir

794 fluctuation zone of the Three Gorges Reservoir, China, Science of the Total
795 Environment, 548-549: 410-420, https://doi.org/10.1016/j.jenvman.2017.08.006,
796 2016.
797 Thomas, M. C. and Scott A. W.: CE-QUAL-W2: A two-dimensional laterally
798 averaged hydrodynamic and water quality model, Version 3.6, Department of
799 Civil and Environmental Engineering, Portland State University, Portland, 2008.
800 Wang, Q.: Influence on fishes of dissolved gas supersaturation caused by high-dam
801 discharging and its countermeasures, Proceedings of 2011 International
802 Symposium on Water Resource and Environmental Protection, Xi'an,
803 https://doi.org/10.1109/ISWREP.2011.5893398, 2011.
804 Wang, R., Huang, T. and Wu, W.: Different factors on nitrogen and phosphorus
805 self-purification ability from an urban Guandu-Huayuan river, Journal of Lake
806 Sciences, 28(1), 105-113, https://doi.org/10.18307/2016.0112, 2016.
807 Wang, Z., Liu, Y., Qin, C., and Zhang, W.: Study on characteristics of hydrodynamic
808 and pollutant transport of the tributary estuary in the three gorges reservoir area,
809 Applied Mechanics & Materials, 675-677, 912-917,
810 https://doi.org/10.4028/www.scientific.net/amm.675-677.912, 2014.
811 Wu, W.: Change of Channel Conditions of the Reach from Wanzhou to Fuling in the
812 Yangtze River at Incipient Stage of Three Gorges Reservoir, Journal of Chongqing
813 Jiaotong University (Natural Science), 32(3), 475-479 (in Chinese),
814 https://doi.org/10.3969/j.issn.1674-0696.2013.03.25, 2013.

Xiong, C., Liu, D., Zheng, B., Zhang, J., Hu, N., Zhang, Y. and Chen, Y.: The Influence of Hydrodynamic Conditions on Algal Bloom in the Three Gorges Reservoir Tributaries, Applied Mechanics and Materials, 295-298, 1981-1990, https://doi.org/10.4028/www.scientific.net/amm.295-298.1981, 2013.

Yang, Z., Cheng, B., Xu, Y., Liu, D., Ma, J. and Ji, D.: Stable isotopes in water indicate sources of nutrients that drive algal blooms in the tributary bay of a subtropical reservoir, Science of The Total Environment 634, 205-213, https://doi.org/10.1016/j.scitotenv.2018.03.266, 2018.

Yang, Z., Liu, D., Ji, D. and Xiao, S.: Influence of the impounding process of the Three Gorges Reservoir up to water level 172.5 m on water eutrophication in the Xiangxi Bay, Science China Technological Sciences 53(4), 1114-1125, https://doi.org/10.1007/s11431-009-0387-7, 2010.

Yang, Z., Liu, D., Ji, D., Xiao, S., Huang, Y. and Ma, J.: An eco-environmental friendly operation: an effective method to mitigate the harmful blooms in the tributary bays of Three Gorges Reservoir, Science China (Technological Sciences), 56, 1458-1470, https://doi.org/10.1007/s11431-013-5190-9, 2013.

Yao, X., Liu, D., Yang, Z., Ji, D. and Fang, X.: Preliminary Studies on the Mechanism of Winer Dinoflagellate Bloom in Xiangxi Bay of the Three Gorges Reservoir, Research of Environmental Sciences, 25(6), 645-651 (in Chinese), https://doi.org/10.13198/j.res.2012.06.40.yaoxj.001, 2012.

Yin, W., Ji, D., Hu, N., Xie, T., Huang, Y., Li, Y. and Zhou J.: Three-dimensional

836 Water Temperature and Hydrodynamic Simulation of Xiangxi River Estuary,
837 Advanced Materials Research, 726-731(2013), 3212-3221,
838 https://doi.org/10.4028/www.scientific.net/AMR.726-731.3212, 2013.
839 Yu, Z., Wang, L., Zhang, L., Yang Y., Yan, L., Zhang, J. and Yang, Y.: Hydrodynamic
840 characteristics in a valley type tributary bay during the raising and falling
841 temperature periods, Applied Mechanics and Materials, 353-356(2013),
842 2567-2571, https://doi.org/10.4028/www.scientific.net/AMM.353-356.2567,
843 2013.
844 Zeng, M., Huang, T., Qiu, X., Wang, Y., Shim J., Zhou, S. and Liu, F.: Seasonal
845 Stratification and the Response of Water Quality of a Temperate
846 Reservoir—Zhoucun Reservoir in North of China, Environmental Science, 37(4):
847 1337-1344 (in Chinese), https://doi.org/10.13227/j.hjkx.2016.04.019, 2016.
848 Zhang, H.: Ways to effectively improve the design level of water conservancy and
849 hydropower projects, China Science and Technology Information 5, 89-90 (in
850 Chinese), https://doi.org/10.3969/j.issn.1001-8972.2014.05.024, 2014.
851 Zhang, S., Song, D., Zhang, K., Zeng, F. and Li, D.: Trophic status analysis of the
852 upper stream and backwater area in typical tributaries, Three Gorges Reservoir,
853 Journal of Lake Sciences, 22 (2), 201-207 (in Chinese),
854 https://doi.org/10.1017/S0004972710001772, 2010.
855 Zhao, Y.: Study on the Influence of Mainstream of the Three Gorges Reservoir on
856 Water Quality of Daning River Backwater Area. Ph.D, Tsinghua University, 2017.

857 Zhao, Y., Zheng, B., Wang, L., Qin, Y., Li, H. and Cao, W.: Characterization of
858 Mixing Processes in the Confluence Zone between the Three Gorges Reservoir
859 Mainstream and the Daning River Using Stable Isotope Analysis, Environment
860 Science & Technology, 50(18), 9907-9914, https://doi.org/
861 10.1021/acs.est.5b01132, 2015.
862 Zheng, B., Zhao, Y., Qin, Y., Ma, Y. and Han, C.: Input characteristics and sources
863 identification of nitrogen in the three main tributaries of the Three Gorges
864 Reservoir, China, Environmental Earth Sciences, 75(17, 1219.1-1219.10.,
865 https://doi.org/10.1007/s12665-016-6028-0, 2016.
866 Zheng, T.: The Study of Water Environment and Sedimentation Regimes in the Upper
867 Three Gorges Reservoir. Proceedings of 2011 International Symposium on Water
868 Resource and Environmental Protection, Xi'an,
869 https://doi.org/10.1109/ISWREP.2011.5893641, 2011.
870 Zheng, T., Mao J., Dai H. and Liu D.: Impacts of water release operations on algal
871 blooms in a tributary bay of Three Gorges Reservoir, Science China
872 (Technological Sciences), 54(6), 1588-1598,
873 https://doi.org/10.1007/s11431-011-4371-7, 2011.
874 Zhou, J., Zhang M. and Lu, P.: The effect of dams on phosphorus in the middle and
875 lower Yangtze river, Water Resource Research, 49, 3659-3669,
876 https://doi.org/10.1002/wrcr.20283, 2013.
877 Zhu, S.: Preliminary Study on Physical Characteristics of Sediment Deposition in the

878 Three Gorges Reservoir, MA.Sc. Changjiang River Scientific Research Institute
879 (in Chinese), 2017.
880 Ziv, G., Baran, E., Nam, S., Rodriguez-Iturbe, I. and Levin, S. A.: Trading-off fish
881 biodiversity, food security, and hydropower in the Mekong River Basin,
882 Proceedings of the National Academy of Sciences of the United States of America,
883 109 (15), 5609-5614, https://doi.org/10.1073/pnas.1201423109, 2012.
884 Zou, J. and Zhai, H.: Impacts of Three Gorges Project on water environment and
885 aquatic ecosystem and protective measures, Water Resources Protection, 32(05),
886 136-140 (in Chinese), https://doi.org/10.3880/j.isssn.1004-6933.1016.05.025,
887 2016.